α-Actinin-1 promotes activity of the L-type Ca^{2+} Channel $Ca_V1.2$

Matthew Turner[1$], David E. Anderson[1$], Peter Bartels[2$], Madeline Nieves-Cintron[2$], Andrea M. Coleman[1,2], Peter B. Henderson[2], Kwun Nok Mimi Man[2], Pang-Yen Tseng[2], Vladimir Yarov-Yarovoy[3], Donald M. Bers[2], Manuel F. Navedo[2], Mary C. Horne[2#], James B. Ames[1#], and Johannes W. Hell[2#]

[1]Department of Chemistry, [2]Department of Pharmacology, and [3]Department of Physiology and Membrane Biology, University of California, Davis, CA 95616, USA.

[$] These authors are equal first authors.
[#] Co-corresponding Authors

Contact information : mhorne@ucdavis.edu ; jbames@ucdavis.edu ; jwhell@ucdavis.edu

Table of Content :

- Appendix Figure S1. Amino acid sequence alignment of $Ca_V1.2$.
- Appendix Figure S2. Isothermal titration.
- Appendix Figure S3. $Ca_V1.2$ mutations that affect α-actinin-1 binding.
- Appendix Figure S4. Structural modeling of the IQ domain of $Ca_V1.2$.
- Appendix Table S1. 95% Confidence intervals (CI).
- Appendix Table S2. 95% Confidence intervals (CI).
- Appendix Table S3. 95% Confidence intervals (CI).
- Appendix Table S4. Oligonucleotides used for QuikChange II mutagenesis.

Appendix Figure S1

[1]*Homo sapiens*,[2]*Pan troglodytes*,[3]*Bos taurus*, [4]*Oryctolagus cuniculus*, [5]*Rattus norvegicus*, [6]*Heterocephalus glaber*, [7]*Mus musculus*, [8]*Danio rerio*, [9]*Drosophila melanogaster*, [10]*Strongylocentrus purpuratus*, [11]*Lymnea stagnalis*, [12]*Caenorhabditis elegans* [13]*Cyanea lamarkii*

Color code of residues: Different from $Ca_v1.2$ | Important for α-actinin binding | Important for α-actinin and CaM binding | Important for apoCaM binding

Appendix Figure S1. Amino acid sequence alignment of the membrane proximal portion of the C-terminal tail of L-type Ca^{2+} channels.

Bold refers to reference sequence (rat $\alpha_1$1.2), turquoise to divergency in amino acid sequence, red to residues K1647 and Y1649, which are important for α-actinin binding only, green to I1654, which is important for both, α-actinin and apoCaM binding, and yellow to F1658 and K1662, which are important for apoCaM binding only. Amino acid sequences were derived from species according to the numerical labeling[1-13]. Data were extracted and compiled from uswest.ensembl.org.

Appendix Figure S2

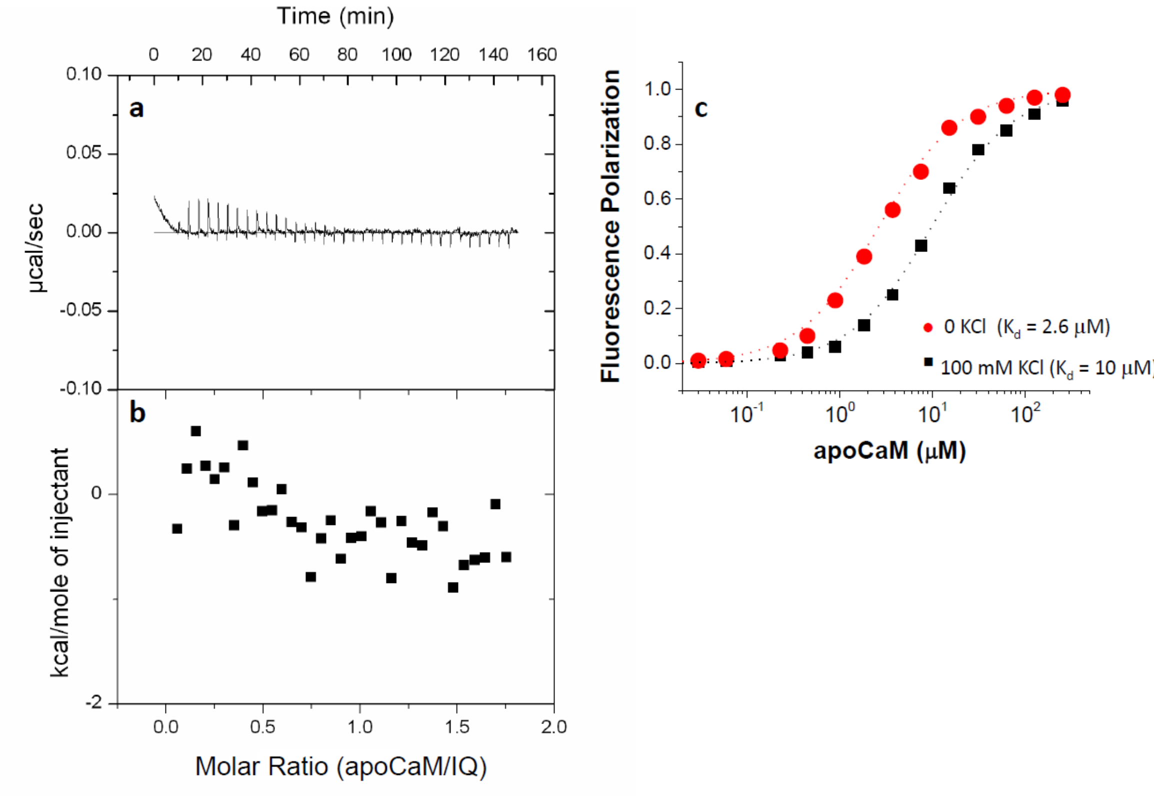

Appendix Figure S2. Isothermal titration calorimetry of apoCaM added to IQ peptide.

a, Change of heat resulting from incremental addition of apoCaM (100 µM stock solution) into IQ peptide (10 µM) during ITC titration at 27°C in 50 mM HEPES (pH 7.4), 100 mM KCl, 0.05 mM EGTA and 1 mM $MgCl_2$.

b, A binding isotherm of apoCaM binding to IQ peptide was derived from the integrated heat at each injection after subtracting a blank titration (to remove heat of dilution). The binding isotherm for apoCaM binding to IQ exhibited no detectable heat signal above the noise level, consistent with low fractional binding under ITC conditions and/or low enthalpy caused by the relatively weak binding affinity (K_d = 10 µM, see Fig. 2e and Table 4).

c, Fluorescence polarization for binding of apoCaM (0.015 to 256 µM) to fluorescein-labeled WT IQ peptide (1.0 µM) in the presence of 100 mM KCl (black squares) versus zero KCl (red dots) at room temperature. The buffer was the same as in (a) except that KCl was excluded in the zero KCl sample. The data were fit to a one-site model (dotted lines) with K_d = 10 µM in the presence of 100 mM KCl and K_d = 2.6 µM in the absence of KCl.

Appendix Figure S3

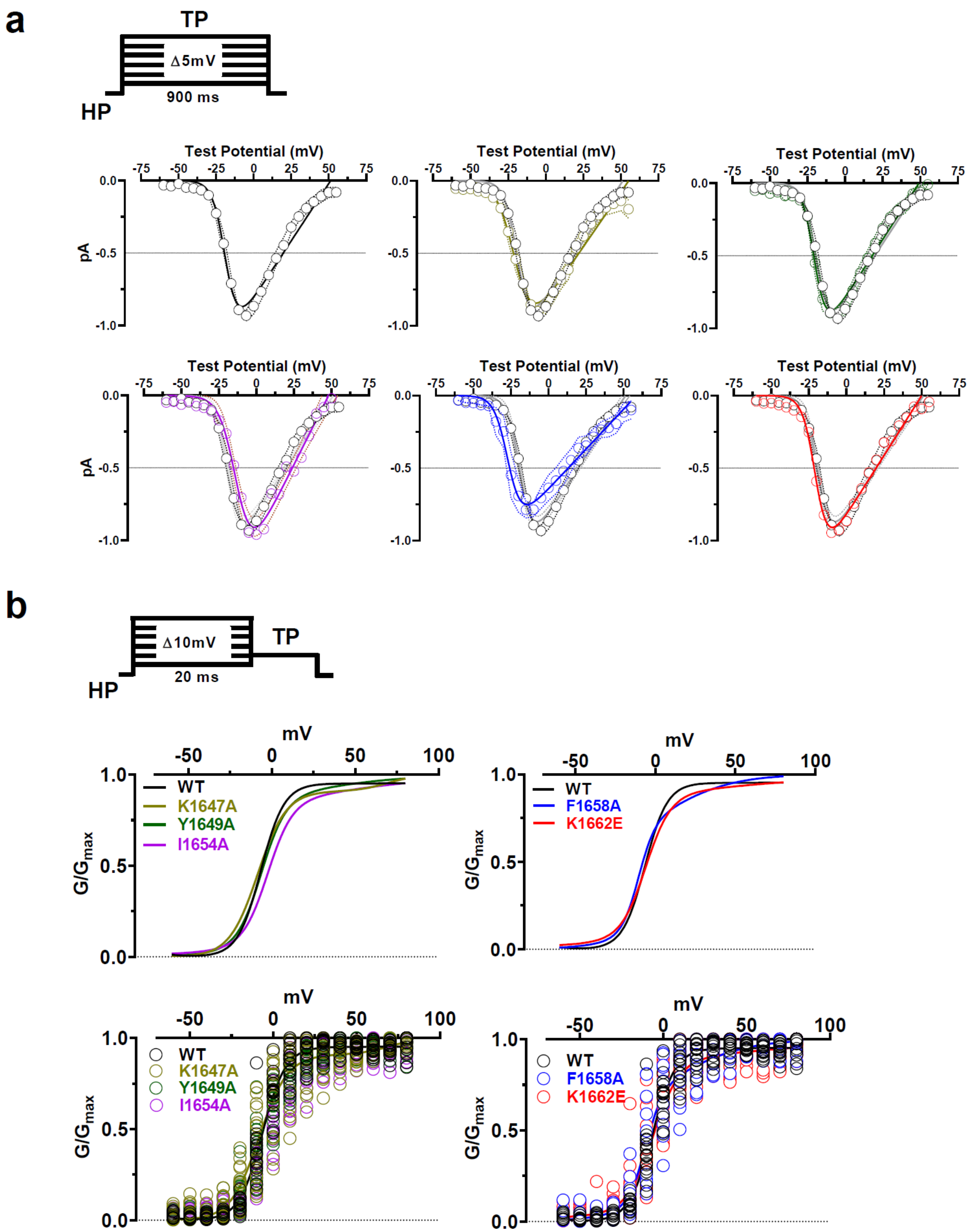

Appendix Figure S3. Cav1.2 mutations that affect α-actinin-1 binding do not impair voltage sensitivity of channel activation.

HEK293 cells were transfected with $\alpha_1$1.2, $\alpha_2\delta$-1, and β_{2A} before whole cell patch recording in 20 mM Ba^{2+}.

a, I-V curves. Currents were recorded upon depolarization from a holding potential of -80 mV to increasingly more positive potentials (insert on left). Shown are peak currents. Dashed lines indicate SEM. The WT Cav1.2 curve is reproduced in all graphs for the Ca_V1.2 mutants.

b, G-V curves. Tail currents (I_{Tail}) were recorded upon repolarization to -50 mV following depolarization from a holding potential of -80 mV to increasingly more positive potentials. Shown are fitted curves in top panels and dot blots in bottom panels.

Appendix Figure S4

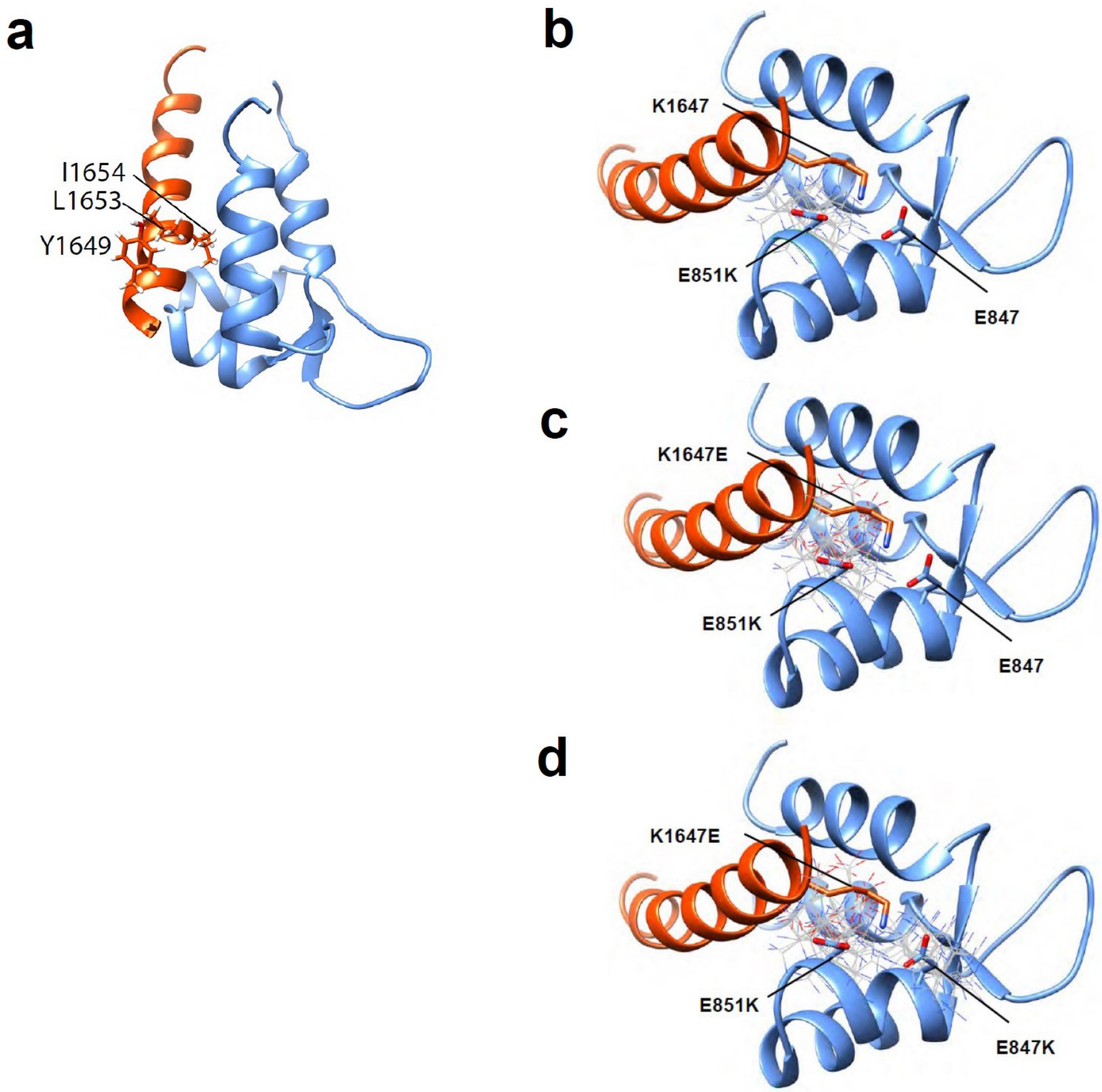

Appendix Figure S4. Structural modeling addressing the function of Y1649 in the $\alpha_1$1.2 IQ motif and how the E851K mutation of α-actinin affects its binding to the IQ motif.

a, Y1649 stabilizes the α-helical conformation of the $\alpha_1$1.2 IQ motif and thereby α-actinin binding. Shown is a cartoon representation of $\alpha_1$1.2 IQ motif α-helix (orange) and α-actinin-1 EF3-EF4 (blue). Sidechains of key residues are depicted as stick representation and labeled. Y1649 is in close proximity to L1653, which is about one α-helical turn downstream of Y1649. Stabilization of this α helix ensures correct positioning of I1654, which is critical for binding to α-actinin. This figure was created using UCSF Chimera (Pettersen et al., 2004).

b-d, The lysine residue in the E851K mutation of α-actinin destabilizes the canonical EF hand structure. Conformers of the lysine residues when used to substitute E851 by itself or together with E847 in α-Actinin-1 and of the glutamate residue when used to substitute K1647 in the IQ motif were calculated for the structure of the complex between the IQ motif of $\alpha_1$1.2 and EF3_EF4 of α-Actinin-1 using the UCSF Chimera rotamer tool (Pettersen et al., 2004). The $\alpha_1$1.2 IQ α-helix is shown in orange and the α-actinin-1 EF3-EF4 in blue. Sidechains of key residues are depicted as stick representation and labeled. The lysine rotamers (thin sticks) are overlaid on top of the original E851 and E847 residues and the glutamate rotamers on top of the original K1647 residue.

b, Simulation of rotamers for the E851K mutation in α-actinin-1 to show possible conformations of the lysine sidechain.

c, Simulation of rotamers for the E851K mutation in α-actinin-1 and the K1647E mutation in $\alpha_1$1.2 to show possible conformations of the lysine and glutamate sidechains.

d, Simulation of rotamers for the E847K and E851K mutations in α-actinin-1 and the K1647E mutation in $\alpha_1$1.2 to show possible conformations of the lysine and glutamate sidechains.

Appendix Table S1. 95% Confidence intervals (CI) for surface labelling, Qon, and Po for WT and IQ mutant Cav1.2

Given are means±SEM and 95% CIs for experimental values. The number of experiments is shown in parenthesis. *The biotinylation and flow cytometry data are based on data originally published by Tseng et al (2017).

Parameter	*Biotin-ylation (% of WT)	95% CI	*Flow Cytometry (% of WT)	95% CI	Gating Current Qon (% of WT)	95% CI	P_{open} (% of WT)	95% CI
α1.2 WT	100±0 (16)	0-0	100±0 (7)	0-0	100±24 (18)	78-122	100±20 (35)	87-113
K1647A	61±5 (11)	52-69	61±7 (7)	51-71	35±9 (15)	26-44	8±2 (12)	6-10
F1648A	94±7 (8)	85-104	ND		ND		93±20 (14)	73-114
Y1649A	66±5 (12)	61-72	63±7 (6)	52 - 74	26±8 (13)	18-35	15±5 (8)	8-22
I1654A	68±4 (10)	63-73	61±8 (6)	49-74	23±10 (13)	1 -34	10±5 (7)	3-17
Q1655A	85±5 (7)	78-92	104±6 (4)	93-116	ND		ND	
F1658A	ND		ND		76±16 (13)	59-93	139±64 (12)	45-121
K1662E	ND		ND		93±29 (17)	52-134	120±32 (13)	86-154

Appendix Table S2. 95% Confidence intervals (CI) for surface biotinylation for Cav1.2 / α-actinin-1 charge inversion experiments

Given are means±SEM and 95% CIs (based on original data from this manuscript). The number of experiments is shown in parenthesis.

Parameter	Biotinylation (%)	95% CI
$\alpha_1$1.2 WT	100±6 (7)	86-114
$\alpha_1$1.2 WT + α-Actinin WT	153±6 (7)	139-167
$\alpha_1$1.2WT+ α-Actinin WT	100±9 (5)	74-126
$\alpha_1$1.2 WT + α-Actinin EE/KK	48±9 (5)	24-72
$\alpha_1$1.2 K1647E + α-Actinin WT	60±5 (5)	47-73
$\alpha_1$1.2 K1647E + α-Actinin EE/KK	55±5 (4)	39-71

Appendix Table S3. 95% Confidence intervals (CI) for Po for Ca_V1.2 / α-actinin-1 charge inversion experiments

Given are means±SEM and 95% CIs (based on original data from this manuscript). The number of experiments is shown in parenthesis.

Parameter	P_{open} (%)	95% CI
$\alpha_1$1.2 WT	100±20 (35)	87-113
$\alpha_1$1.2 WT + α-Actinin WT	233±59 (23)	186 - 280
$\alpha_1$1.2 WT+ α-Actinin EE/KK	55±22 (13)	32-78
$\alpha_1$1.2 K1647E + α-Actinin WT	100±18 (30)	87-113
$\alpha_1$1.2K1647E + α-Actinin EE/KK	147±28 (16)	120-174

Appendix Table S4. Oligonucleotides used for QuikChange II mutagenesis.

Cav1.2/ α-Actinin-1	Used primers
	Primer (Forward/Reverse; Bold type indicates mutated nucleotide)
RtBr-Cav1.2-a1c-K1647E-Forw	5' – CGA GGT CAC AGT GGG C**G**A ATT CTA TGC CAC CTT C – 3'
RtBr-Cav1.2-a1c-K1647E-Rev	5' – GAA GGT GGC ATA GAA TT**C** GCC CAC TGT GAC CTC G – 3'
RtBr-Cav1.2-a1c-K1662-Forw	5' – CAA GAG TAC TTC AGG AAA TTC **G**A**A** AAG CGA AAA GAG CAG GGG CTG – 3'
RtBr-Cav1.2-a1c-K1662-Rev	5' – CAG CCC CTG CTC TTT TCG CTT **T**T**C** GAA TTT CCT GAA GTA CTC TTG – 3'
Hum-ACTN-1-E847K-Forw	5' – GAA CTA CAT TAC CAT GGA C**A**A **A**TT GCG CCG CGA GCT GCC ACC C – 3'
Hum-ACTN-1-E847K-Rev	5' – GGG TGG CAG CTC GCG GCG CAA **T**T**T** GTC CAT GGT AAT GTA GTT C – 3'
Hum-ACTN-1-E847KE851K-Forw	5' – CCA TGG AC**A** A**A**T TGC GC**A** G**AA** AGC TGC CAC CCG ACC AGG – 3'
Hum-ACTN-1-E847KE851K-Rev	5' – CCT GGT CGG GTG GCA GCT **TT**C **T**GC GCA A**T**T **T**GT CCA TGG – 3'